Error Analysis of a Parallel Mechanism Considering Link Stiffness and Joint Clearances

Seung Reung Lim, Kyungwoo Kang, Sungchul Park
Graduate Students, Department of Mechanical Engineering, Korea University, Seoul 136-701, Korea
Woo Chun Choi*, Jae-Bok Song, Daehie Hong, Jae Kyung Shim
Department of Mechanical Engineering, Korea University, Korea University, Seoul 136-701, Korea

In order to utilize a parallel mechanism as a machine tool component, it is important to estimate the errors of its end-effector due to the uncertainties in parts. This study proposes an error analysis for a new parallel device, a cubic parallel mechanism. For the parallel device, we consider two kinds of errors. One is a static error due to link stiffness and the other is a dynamic error due to clearances in the parts. In this study, we propose a stiffness model for the cubic parallel mechanism under the assumption that the link stiffness is a linear function of the link length. Also, from the fact that the errors of u-joints and spherical joints are changed with the direction of force acting on the link, they are regarded as a part of link errors, and then the error model is derived using forward kinematics. Lastly, both the error models are integrated into the total error, which is analyzed with a test example that the platform moves along a circular path. This analysis can be used in predicting the accuracy of other parallel devices.

Key Words : Parallel Manipulator, Stiffness, Error Analysis, Position Error, Orientation Error

1. Introduction

There has been researches in which parallel-structured mechanisms are utilized for machine tools. Those parallel-structured devices consist of a fixed base, a moving platform, and more than two serial links that form a closed chain and restrict the motion of the base and the platform. All of those parts constrain the relative motion among them, so they can have higher accuracy than serial-structured devices.

Open-chained serial mechanisms have a large workspace and they are used for tasks requiring flexible motions. However, they are greatly affected by inertia force, centrifugal force, and gravity force. Also, their joint errors are accumulated, which results in large errors in the moving platform. On the other hand, although parallel structured device has a relatively small workspace and little flexibility, it forms a closed chain, and thus the errors of parts are not accumulated.

Because of these merits of the parallel mechanisms, there have been many studies to utilize them for machine tools. Masory and Wang (1993) discussed the effect of manufacturing tolerances, installation errors, and link tolerances to set up an error model of general type parallel manipulators. Ehmann and Patel (1997) developed an error model based on differentiation of kinematic equations. Wang and Ehmann (1995) investigated and proposed a model on a link component which has one degree of freedom, and induced ball joint errors by using D-H transformation. Satori and Zhang (1995)

* Corresponding Author,
E-mail : wcchoi@korea.ac.kr
TEL : +82-2-3290-3761; **FAX** : +82-2-926-9290
Department of Mechanical Engineering, Korea University 5-1 Anam-dong, Sungbuk-ku, Seoul 136-701, Korea. (Manuscript **Received** August 9, 2001; **Revised** February 21, 2002)

studied a method of geometric error evaluation and generalization of errors. Ropponen and Arai (1995) presented the relation between joint displacement errors of Stewart platform manipulators and end-effector accuracy.

Also, there have been studies on the stiffness that can affect the errors in parallel mechanisms. Gosselin (1990) calculated the stiffness of Stewart Platform under the assumption that the stiffness of each link is the same regardless of change in the link length. El-Khasawneh and Ferreira (1999) studied stiffness range and direction using eigen values. However, there have been few researches concerning the joint clearance and the direction of force acting on links with the error of the end-effector accuracy. Furthermore, on the analysis of error of the end-effector pose on the parallel manipulator, it is really required to synthesize the joint errors and link stiffness: both are the main error sources of the end-effector. Until now the research on the errors of the cubic parallel manipulator, which includes both the joint errors and the link stiffness, has not been reported in the literature.

In order to predict errors precisely, we formulate the stiffness of the whole mechanism with the stiffness of each link considered. In this study, the stiffness of a link is obtained from material properties of all the parts of the link under the assumption that there is no clearance. After achieving a stiffness matrix for the whole parallel mechanism, one can find the errors at a specific position using Jacobian transformation and vector calculus.

However, in real situation, joint clearances should be considered, since especially the clearances of u-joints and spherical joints can greatly influence the accuracy of the moving platform. They can be determined by the force direction on each link when the platform is driven and they can be regarded as a part of link error.

In this study, we propose a stiffness model for a cubic parallel mechanism using ABAQUS under the assumption that the stiffness of each link is a linear function of the link length. Then, the errors of the end-effector are calculated from the stiffness model. Also, from the fact that the error of an u-joint is changed with the direction of force acting on the link, we regard the u-joint errors and spherical joint errors as a part of link errors, and make a model using forward kinematics. At the end, we suggest a complete model that consists of a stiffness error model and a joint error model, and show error results from a simulation test that the platform moves along a circular path.

2. Configuration of Parallel Mechanism and Its Kinematics

2.1 Configuration of cubic parallel manipulator

The parallel manipulator used in this study is supported by three links in the direction of Z-axis, two links in the direction of X-axis, and one link in the direction of Y-axis, as shown in Fig. 1. Each link is composed of a ball-screw and a nut, and is connected to a universal joint and a spherical joint at its both ends. The length of the link changes by the translation movement by ball-screw revolution. All the six links are installed between the base and the moving platform. By changing the length of the links in the direction of Z-axis, translation motion to the Z-axis and rotation motion about Y-axis can be achieved. With the length of the two links in the direction of X-axis changing translation motion

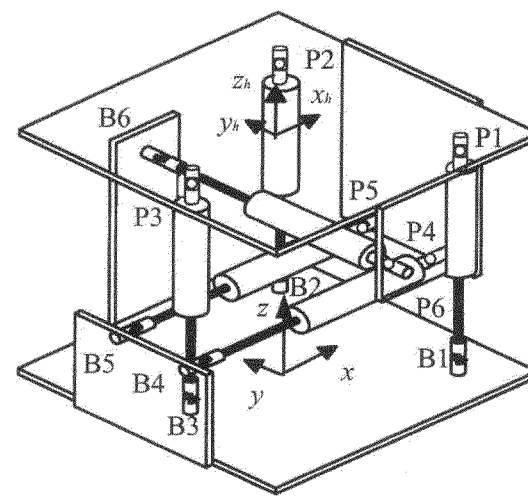

Fig. 1 A proposed cubic parallel manipulator

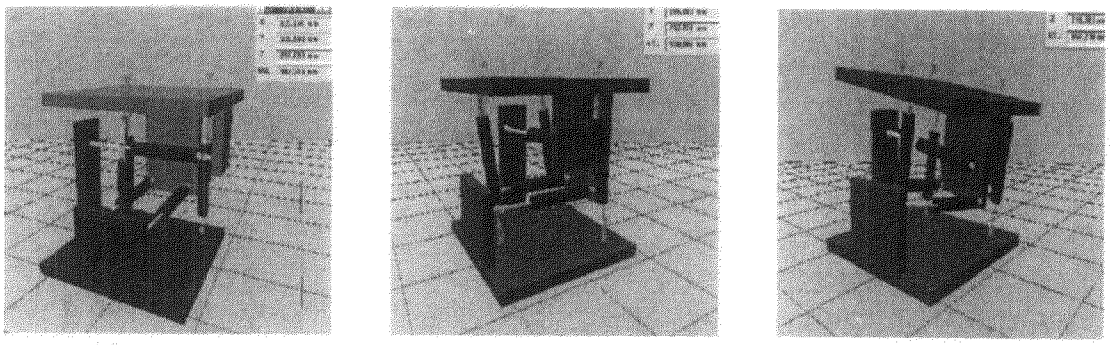

(a) Initial state (b) Translation (x-direction) (c) Rotation (x-direction)

Fig. 2 Motion of cubic parallel manipulator

to the X-axis and rotation motion about Z-axis can be achieved, as shown in Fig. 2. Also, with the length of one link in the direction of Y-axis changing, translation motion to the Y-axis and rotation motion about X-axis or about Z-axis can be achieved.

The presented device has some different features compared to the other types of parallel manipulators that have been studied. Most of all, only three links to the Z-axis mainly bear the weight of the moving platform, and thus the presented device might have less stiffness than the general type of the parallel manipulator. However, by changing of the length of each link, we can easily make the translation motions to the three axes. In other words, if we make a desired motion of the general type of the parallel manipulator, we must solve the complicated forward kinematics of the six links, but for the cubic parallel manipulator we just need to solve the simple arithmetic problems. For example, to get the displacement to Z-axis of the end-effector, we can increase the length of the three links in the direction of Z-axis, and solve the simple equations composed of a few trigonometric functions to find the changed length of two links to X-axis and the changed length of the Y-directional link. Thus, we can easily control the path of end-effector in real time.

2.2 Inverse kinematics

Figure 3 illustrates some definitions of kinematic parameters of the proposed cubic parallel manipulator. Each link has a spherical joint

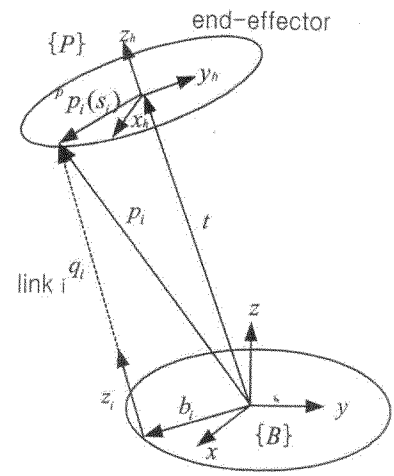

Fig. 3 Kinematic parameters of a link

connected to a mobile platform, a linear actuator, and a universal joint connected to the base. Two Cartesian coordinate systems are used, the moving frame (x_h, y_h, z_h) attached to the mobile platform and the fixed frame (x, y, z) attached to the base as shown in Fig. 3. ${}^p p_i$ denotes the position of the center of the universal joint connected to the i^{th} link from the moving platform frame. R is the rotational matrix expressing the orientation of the moving frame with respect to the fixed base frame.

With the rotational matrix R, ${}^p p_i$ can be defined with respect to the base frame.

$$s_i = R\,{}^p p_i \tag{1}$$

From the geometry of the manipulator, the link vector q_i, with respect to the base frame, is expressed as

$$q_i = t + s_i - b_i \tag{2}$$

where t is the position of the moving frame origin and b_i represents the position of the universal joint center (connected to the i^{th} link) from the base frame center.

The link vector q_i is equal to the link length l_i times unit vector z_i in the link direction.

$$q_i = l_i z_i \tag{3}$$

Substituting Eqs. (1) and (3) into Eq. (2), the following expression is obtained

$$l_i z_i = t + R^p p_i - b_i \tag{4}$$

2.3 Jacobian

The following equation represents the relation between the external force exerted on the platform and the link actuator force τ.

$$F = J^T \tau,\ \tau = [\tau_1,\ \tau_2,\ \cdots,\ \tau_6]^T \in \mathscr{R}^{6\times 1} \tag{5}$$

where the Jacobian can be expressed as

$$J^T = \begin{bmatrix} z_1 & \cdots & z_6 \\ s_1 \times z_1 & \cdots & s_6 \times z_6 \end{bmatrix} \in \mathscr{R}^{6\times 6} \tag{6}$$

In Eq. (5), τ represents the force vector acting on the links, and F represents forces and moments.

3. Stiffness Error Model

The relation between the change in the location of the moving platform and in the link length can be written as

$$\Delta q = J \Delta x_s \tag{7}$$

where Δq denotes the change in the link length, denotes the change in the platform position, and J is the Jacobian matrix.

The actuating force on each link can be written as

$$\tau = diag[k_i] \Delta q \tag{8}$$

where k_i denotes the stiffness of the th link. To find the stiffness of the th link, we make a FEA model using ABAQUS as shown in Fig. 4. Each link is composed of a ball-screw and a nut and is connected to a universal joint and a spherical joint at its both ends, and the physical properties of one link are shown in table 1. To find the maximum and minimum stiffness, we can get the displacement of each link when a compression force (210N) is applied.

Table 1 Physical properties of a link

Material	Young's modulus(E)	Poisson's ratio(ν)
Aluminum	73GPa	0.33
Steel	200Gpa	0.25

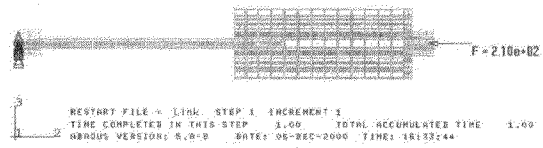

Fig. 4 A proposed cubic parallel manipulator

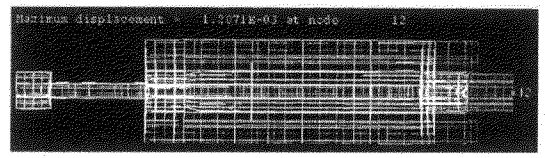

Fig. 5 FEA result of the deformed link of minimum link (L=404mm, k_1=8.288×10^{10}N/m)

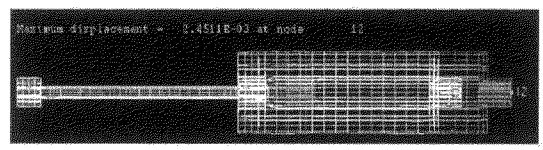

Fig. 6 FEA result of the deformed link of maximum link (L=279mm, k_2=4.080×10^{10}N/m)

Figures 5 and 6 show the displacements of each link and also we can find the maximum and minimum stiffness, respectively. The stiffness of the th link is given by the following equation, when it is assumed to be a linear model,

$$k_i = \frac{(L_i - L_i)(k_{L_1} - k_{L_2})}{(L_1 - L_2)} + k_{L_2} \tag{9}$$

where L_2 is the maximum length of the link, and L_1 is the minimum length. k_{L_1} is the stiffness when L_i is equal to L_1, and k_{L_2} is the stiffness when L_i is equal to L_2.

From Eqs. (5) and (9), F can be expressed as

$$F = J^T diag[k_i] \Delta q \tag{10}$$

where $diag[k_i]$ can be defined as follow.

$$diag[k_i] = \begin{bmatrix} k_1 & 0 & \cdots & 0 \\ 0 & k_2 & \cdots & 0 \\ \vdots & \vdots & \ddots & \vdots \\ 0 & 0 & \cdots & k_6 \end{bmatrix} \in \mathscr{R}^{6\times 6} \tag{11}$$

The stiffness equation of the mechanism is given by

$$F=K\Delta x_s \tag{12}$$

From Eqs. (6) and (11), K can be obtained as

$$K=J^T diag[k_i]J \tag{13}$$

When an external force is exerted on the moving platform, the link forces acting in the longitudinal direction can be calculated from Eq. (5). If the external force and the link stiffness are given, we can find the error of the end-effector Δx_s. The deformation of the mechanism is directly influenced by the components of the stiffness matrix K. Consequently, Δx_s can be obtained using the following equation.

$$\Delta x_s=K^{-1}\Delta F \tag{14}$$

4. Error Analysis Using Forward Kinematics

4.1 Inverse kinematics and rotational matrix

Inverse kinematics is posed as follows: given the position and orientation of the end-effector of the manipulator, calculate all the possible sets of joint variables.

The cubic parallel manipulator consists of 6 links, each of which is connected to the base and the end-effector, respectively. The base is expressed with respect to the fixed coordinate system (x, y, z), and the platform is defined with respect to the moving coordinate system (x_h, y_h, z_h).

The rotational matrix, R, defines the orientation of the platform relative to the base.

$$R=\begin{bmatrix} C_\gamma C_\beta & C_\gamma S_\beta S_\alpha - S_\gamma C_\alpha & C_\gamma S_\beta C_\alpha + S_\gamma S_\alpha \\ S_\gamma C_\beta & S_\gamma S_\beta S_\alpha + C_\gamma C_\alpha & S_\gamma S_\beta C_\alpha - C_\gamma S_\alpha \\ -S_\beta & C_\beta S_\alpha & C_\beta C_\alpha \end{bmatrix} \tag{15}$$

The rotational matrix is correct only for the rotations performed in the following order: about x-axis by α, about y-axis by β, and about z-axis by γ.

Link length (L_i) is defined as (see Fig. 3)

$$L_i=|\,q_i\,|=|\,l_i z_i\,|=|\,t+R^p p_i-b_i\,| \tag{16}$$

Equation (16) represents the i^{th} link length referenced to the base coordinate system. The link length is defined by the distance between the centers of joints on the platform and the base.

4.2 Forward kinematics

Forward kinematics is posed as follows: given all the sets of joint variables, calculate position and orientation of the end-effector of the mechanism.

Since the cubic parallel manipulator forms a closed chain, there exist passive joints and the kinematics can be defined by an implicit function. This study does not deal with the forward kinematics of a special form of parallel manipulator but tries to solve forward kinematics by using a general method when initial position is given.

The following implicit function can be derived from Eq. (16).

$$L_i-|\,t+R^p p_i-b_i\,|=0 \tag{17}$$

and,

$$L_i^2-(t+R^p p_i-b_i)^T(t+R^p p_i-b_i=0) \tag{18}$$

By expanding Eq. (18) and introducing a scalar function, Eq. (18) can be written as

$$\begin{aligned} f_i=&L_i^2-t^T t-2t^T R^p p_i+2t^T b_i+\\ &2b_i^T\,{}^p R p_i-p_i^T\,{}^p R^T R p_i-b_i^T b_i=0 \end{aligned} \tag{19}$$

where the subscript i denotes the i^{th} link. If all the link lengths L_i are given, the translation t and the orientation R of the end-effector can be determined.

In order to find the solutions for these nonlinear simultaneous equations, a multi-variable Newton-Raphson method can be used if the solutions are in the range of workspace that has no singular points. First, we define a vector X that consists of the position and the orientation of the end-effector;

$$X=\{\,t^T\{\,\alpha\quad\beta\quad\gamma\,\}^T\}^T \tag{20}$$

A new X can be calculated as follows:

$$X_{new}=X_{old}-\delta X=X_{old}-J^{-1}\delta F \tag{21}$$

In Eq. (21), J is defined as $\frac{\partial f_i}{\partial X_j}$, and δF is the vector $\{\,\delta f_1\cdots\delta f_6\,\}^T$. To calculate Eq. (21), we have to investigate the components of J,

$$J=[J_1 \quad J_2 \quad J_3 \quad J_4 \quad J_5 \quad J_6]^T \tag{22}$$

where $J_i=\left[\frac{\partial f_i}{\partial x}, \frac{\partial f_i}{\partial y}, \frac{\partial f_i}{\partial z}, \frac{\partial f_i}{\partial \alpha}, \frac{\partial f_i}{\partial \beta}, \frac{\partial f_i}{\partial \gamma}\right]$

Also, if t is differentiated with respect to x, y, and z, the following equations are obtained

$$\frac{\partial t}{\partial x}=\frac{\partial\{x \quad y \quad z\}}{\partial x}=\{1 \quad 0 \quad 0\}^T, \frac{\partial t^T}{\partial x}=\{1 \quad 0 \quad 0\} \tag{23a}$$

$$\frac{\partial t}{\partial y}=\frac{\partial\{x \quad y \quad z\}}{\partial y}=\{1 \quad 0 \quad 0\}^T, \frac{\partial t^T}{\partial y}=\{0 \quad 1 \quad 0\} \tag{23b}$$

$$\frac{\partial t}{\partial z}=\frac{\partial\{x \quad y \quad z\}}{\partial z}=\{0 \quad 0 \quad 1\}^T, \frac{\partial t^T}{\partial z}=\{0 \quad 0 \quad 1\} \tag{23c}$$

Using equations (20)-(23c), the procedure to find a solution includes the following steps:

① F is calculated with an initial value of X. Then, J is calculated from Eq. (22). At this time L_i, are the given link lengths and the initial values are used to determine t and R. In this case, F is not a zero vector.

② Substituting the new F and J into Eq. (21) gives a new X.

③ Calculate F and J with the new X. At this time, L_i are the updated link lengths, and t and R are obtained with the new X.

④ A tolerance of the norm of F is set. If the norm of F is not within the tolerance, we should go back to step ③, otherwise iteration is stopped, and the final value of X represents the position and orientation of the platform.

⑤ The recent X will be used as an initial point for the next step.

4.3 Error analysis considering joint clearances

The link length is defined as the distance between the center of the universal joint and the center of the spherical joint that are attached to the end of the link. A universal joint has two rods that are assembled into the holes. The rods rotate inside the holes and there exist clearances between them. Because of the clearance, the center of universal joint deviates from an ideal position and this deviation affects the errors of the end-effector. Because the clearance restricts the motion of rods, the center of two rods in the universal joint is located within a sphere as shown in Fig. 7(a). The radius of the sphere is equal to the clearance and it is denoted by c_b. When the platform moves, the actuator forces can be obtained by using Eq. (5). Also, a spherical joint has a clearance that deviates from its ideal center as shown in Fig. 7(b). Because of the deviation, the motion of the spherical joint center is res-

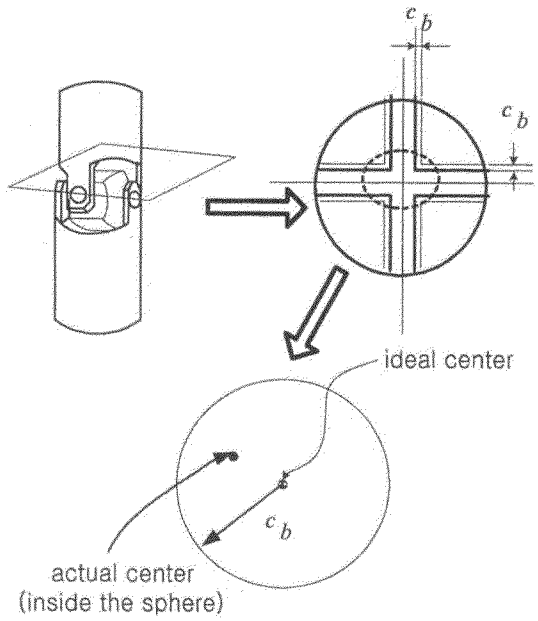

Fig. 7(a) Clearance of a u-joint and position error bound of the joint center

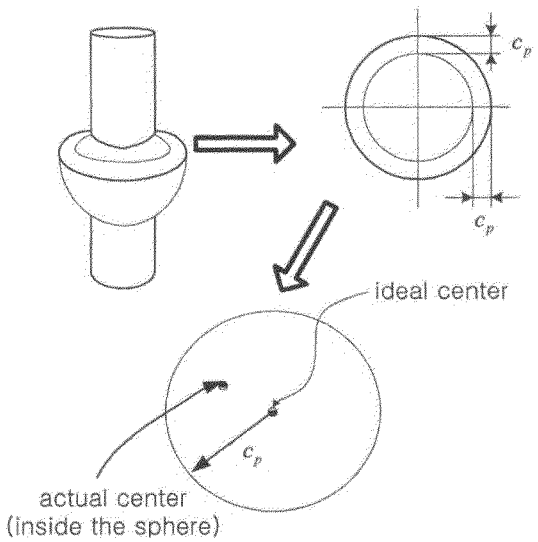

Fig. 7(b) Clearance of a spherical joint and position error bound of the joint center

tricted within a sphere with radius c_p where the subscript p denotes the moving platform.

At the previous research of the error of the parallel manipulator, Tatsuo Arai and Timo Ropponen suggested the joint errors and link length errors could acquire the error of the parallel manipulator. The well-known error equation by them is represented as

$$\delta X = J_1^{-1}\delta l_i - J_1^{-1}J_2\delta p \tag{24}$$

where $J_1=[z_i^T \ (s_i\times z_i)^T]\in\mathscr{R}^{6\times 6}$, $\delta X=\begin{bmatrix}\delta t\\ \delta\Omega\end{bmatrix}\in\mathscr{R}^{6\times 1}$,

$$J_2=[z_i^T R \ -z_i^T]\in\mathscr{R}^{6\times 36},\ \delta p=\begin{bmatrix}\delta^p p_i\\ \delta b_i\end{bmatrix}\in\mathscr{R}^{36\times 1}$$

δX includes the position and orientation errors that are represented as 6×1 vector, and J_1 includes z_i^T (unit link length vectors) and the cross product of $(s_i\times z_i)^T$ as 6×6 square matrix. δl_i is the link length error represented as 6×1 vector, and J_2 includes $z_i^T R$ and $-z_i^T$ expressed as 6×36 matrix. Equation (24) means that we can find the 6 errors of the end-effector (3 position errors and 3 orientation errors) by δl_i (the link length error) and δp (joint error). However Eq. (24) would not be the exact results because the range, direction and magnitude of the joint errors should be assumed. But we suggested the following model to find the much more accurate error model. When the platform moves, the each link have the compression force or tensile force along the link length direction, and the force will determine the size and direction of joint errors if we know the maximum clearance of the universal joints and ball joints.

The relationship between link force (τ_i) and actual link length (l_{ai}) can be expressed

① When τ_i has (+) sign,

$$\begin{aligned} &c_{bUi}=(+)\,c_b z_i,\ c_{pSi}=(-)\,c_p z_i,\\ &l_{ai}=l_{ni}+(c_b+c_p) \end{aligned} \tag{25}$$

② When has (−) sign,

$$\begin{aligned} &c_{bUi}=(-)\,c_b z_i,\ c_{pSi}=(+)\,c_p z_i,\\ &l_{ai}=l_{ni}-(c_b+c_p) \end{aligned} \tag{26}$$

where, c_{bUi} is the motion error vector of a universal joint on the base platform, the c_{pSi} is the motion error vector of a spherical joint on the moving platform and where l_{ai} is an actual link length and l_{ni} is a nominal link length. And the sign of τ_i gives a criterion whether it is a tensile or compression force and it affects the joint error.

The joint errors can be regarded as the part of the link length errors because the directions of the joint errors are the same as those of link length directions. With all these results, we can verify the following equation.

$$\begin{aligned} X_{new}&=X_{old}-\delta X\\ &=X_{old}-J_1^{-1}\delta l_i+J_1^{-1}J_2\delta p \end{aligned} \tag{27}$$

If joint errors are the part of the link errors, δp will be zero. Then we rearrange Eq. (27) as

$$\begin{aligned} X_{new}&=X_{old}-\delta X=X_{old}-J_1^{-1}\delta l_i\\ &=X_{old}-J^{-1}\delta F \end{aligned} \tag{28}$$

That is, the actual link length depends on the direction of force acting on the link.

The u-joint clearance and the spherical joint clearance, which are located on both ends of each link, are included in the link error terms and it changes the third step (③) for finding the solution of the forward kinematics: the real link length (l_{ai}) should be substituted into L_i. After this modification, we can find the exact actual position and orientation of the end-effector.

At the stated third step (③), we substitute into L_i with l_{ni} to find the nominal position and orientation of the end-effector, which does not contain any errors. As such, the difference between the nominal position (and orientation) and the actual position (and orientation) is the error of the end-effector. The result can be expressed as follows.

$$\Delta X=\{\Delta t^T\{\Delta\alpha \quad \Delta\beta \quad \Delta\gamma\}^T\}^T \tag{29}$$

Since the errors due to link compliance (Δx_s in Eq. (14)) and joint clearance (ΔX in Eq. (29)) are independent each other, both can be combined and the total errors of end-effector can be represented as follows.

$$\Delta X_{total}=\Delta x_s+\Delta X \tag{30}$$

5. Case Study

A simulation test is performed with the cubic parallel mechanism. The parameters are given in

Table 2, Table 3, Fig. 8, and Fig. 9.

As the first test, the platform is driven along a circular path (radius of 10cm) with a constant centrifugal acceleration of 10rad/sec^2 on a horizontal plane of z=410mm. The errors are analyzed by considering the directions of actuator link forces. Figures 8 and 9 show the locations of the universal joints and the error spheres. The variables, a, b, c, d, e, f, g, c_b, z_1, z_2, and z_3 can be changed according to design. Then, the magnitudes and directions of forces can be obtained as the platform is moving counter-clockwise along the circular path and the results

Table 2 Kinematic parameter values of cubic parallel mechanism

Weight of platform	47.068N
Cutting force (-z direction)	500N
Clearance of u-joint	10μm
Back-lash error of ball-screw	0μm

Table 3 Coordinates of joint centers

Parameter	Coordinate	Parameter	Coordinate
B1	$(b, -a, 0)$	P1	$(b, -a, 0)$
B2	$(b, a, 0)$	P2	$(b, a, 0)$
B3	$(-b, 0, 0)$	P3	$(-b, 0, 0)$
B4	$(-c, -e, z_1)$	P4	$(c, -e, -d)$
B5	$(-c, e, z_2)$	P5	$(c, e, -d)$
B6	$(0, f, z_3)$	P6	$(0, -f, -g)$

a=0.16m, b=0.14m, c=0.195m, d=0.270m, e=0.055m, f=0.205m, g=0.130m, c_b=0.00001m, c_p=0.00001m, z_1=0.130m, z_2=0.130m, z_3=0.280m

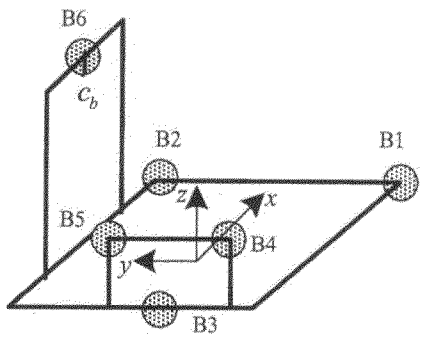

Fig. 8 Effor ranges of u-joint centers on the base

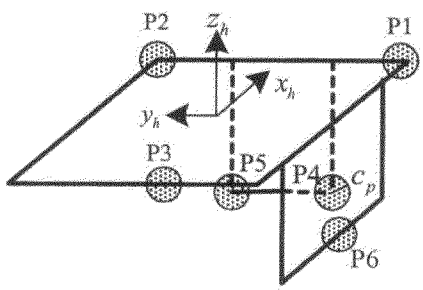

Fig. 9 Error ranges of spherical joint centers on the platform

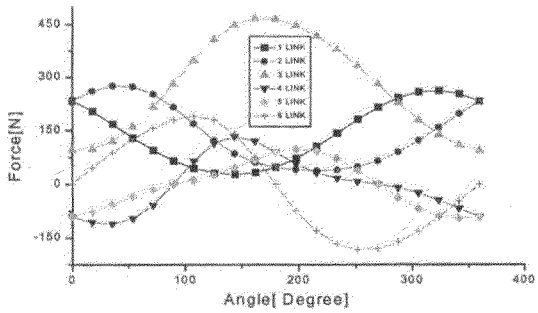

Fig. 10 Actuating link forces

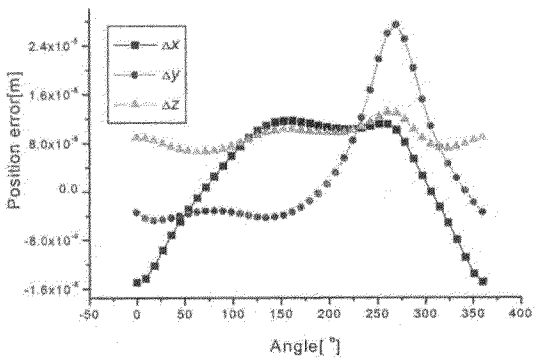

Fig. 11 Position errors by static actuating force

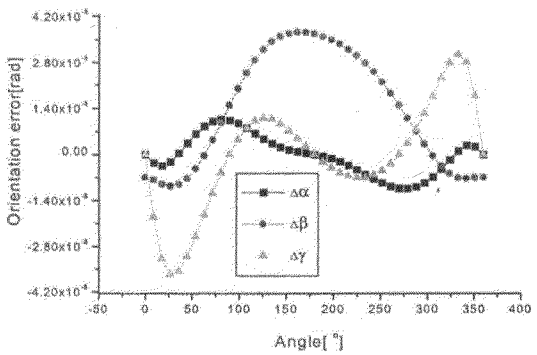

Fig. 12 Orientation errors by static actuating force

are shown in Fig. 10. From the result of Fig. 10, we can find the u-joint errors and they can be substituted into Eqs. (25) and (26) to obtain the link length errors.

The acquired values are substituted into Eq. (19)~Eq. (21) and iterations are carried out until the result converges to a certain limit. Then, the errors of the end-effector that is composed of joint errors can be obtained.

The next step is to find the errors due to the stiffness of links when the platform is moving. They are referred as static errors in this study. At first, the stiffness values of a link are found which includes all the mechanical elements, such as ball screw, nut, and cylindrical cover by using ABAQUS. The maximum stiffness is $k_{L1}=8.288\times10^{10}$N/m at 27.9cm-length of link, and the minimum stiffness is $k_{L2}=4.080\times10^{10}$N/m at 40.4cm-length of link.

Next, the stiffness matrix of whole mechanism is calculated from Eqs. (10)~(13), and substituted into Eq. (14), leading to the error of the

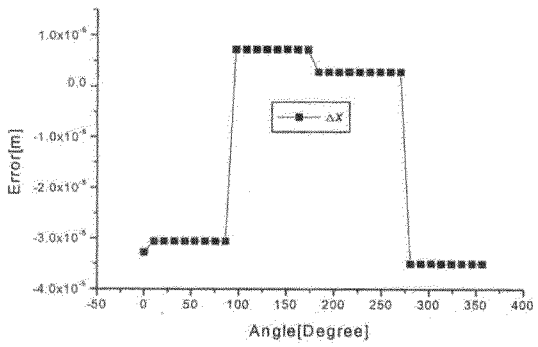

(a) Position error (Δx)

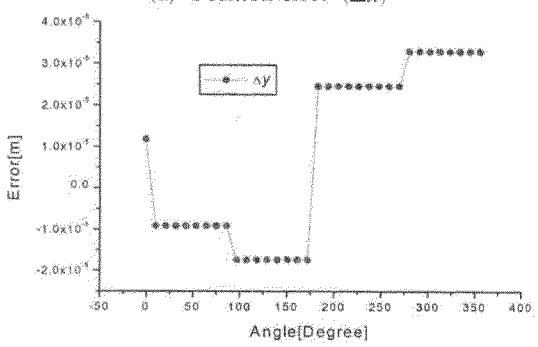

(b) Position error (Δy)

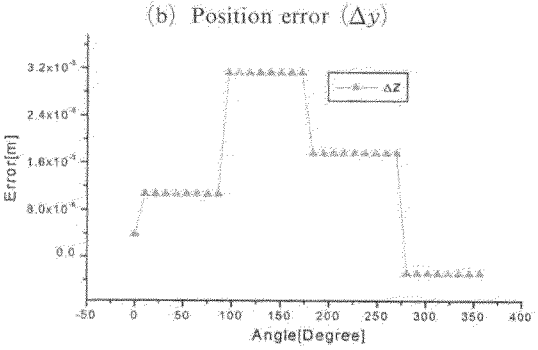

(c) Position error (Δz)

Fig. 13 Total position errors due to link stifness and joint clearances

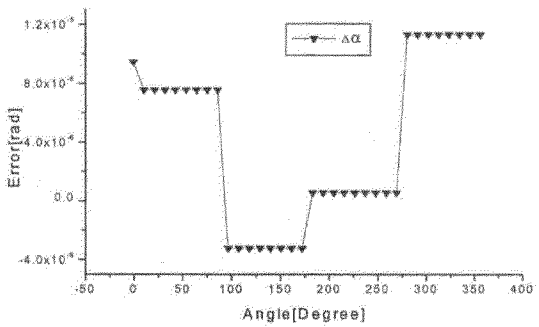

(a) Orientation error ($\Delta\alpha$)

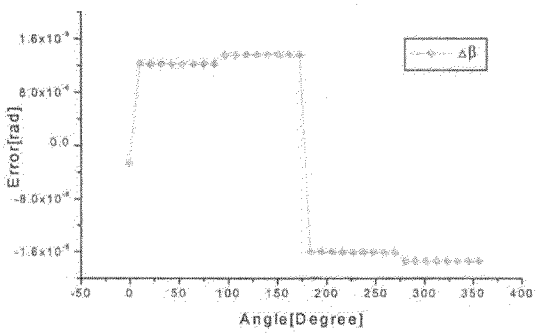

(b) Orientation error ($\Delta\beta$)

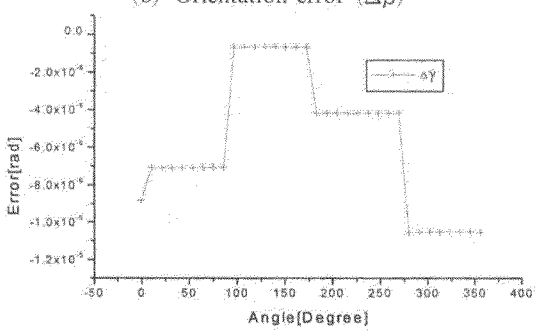

(c) Orientation error ($\Delta\gamma$)

Fig. 14 Orientation errors due to link stiffness and joint clearances

end-effector. These results are shown in Fig. 11 and Fig. 12. As we can see, the error change is inversely proportional to the stiffness of a link in each direction. The largest y position error (Δy) is located at 270° and the largest y orientation error ($\Delta\beta$) is located at 180°.

Lastly, after combining the static and joint errors, we can find the total position errors and orientation errors in the direction of each axis as shown in Fig. 13 and Fig. 14. The fourth and fifth links influence the x-direction position errors (Δx), when the cubic parallel manipulator carries on circular motion. Thus, the values rapidly change at the angles at 90° and 270° where the direction of force changes. Also, the sixth link influences the y-direction position errors (Δy) and the errors rapidly change at the points where the direction of force changes. The first, second, and third links influence the z-direction errors (Δz). The errors rapidly change at the angles of 90°, 180°, and 270°, where the directions of the forces acting on the first, second and third links change, respectively.

As for the orientation errors, the direction of each link is very important. The x-directional orientation errors ($\Delta\alpha$) are mainly influenced by the first and second links. The y-directional orientation errors ($\Delta\beta$) are primarily affected by the first, second and third links. The z-directional orientation errors ($\Delta\gamma$) are mostly influenced by the fourth and fifth links.

A noteworthy point is that the values of the static errors, which are obtained from the link stiffness, are very small compared to the joint errors. This implies that the errors in joints are dominant than others.

6. Conclusions

Errors in the parallel manipulator are classified into two types: the static errors due to link stiffness and the dynamic errors due to joint clearances. In this study, the static errors are calculated from the link stiffness in any orientation of platform. Secondly, we find the equations of variable errors by the link force. Then, we synthesize all the equations to find complete equations for the errors of the platform. Conclusions obtained from the simulation results are summarized as follows:

(1) The position errors and orientation errors are affected by the direction of link forces.

(2) The changes of errors mostly occur at the positions where the directions of exerting link forces shift.

(3) The position of each link and its configuration of the parallel platform determine the maximum errors.

(4) It can be considered that the errors of the end-effector due to link stiffness are relatively small compared to the joint errors.

The presented analysis method can be also utilized in predicting the accuracy of other types of parallel devices.

Acknowledgement

This work was supported by grant number 1999-1-304-003-3 from the Basic Research Program of the Korea Science and Engineering Foundation.

References

Ehmann, K. F. and Patel, A. J. 1997, "Volumetric Error Analysis of a Stewart Platform-Based Machine Tool," *Annals of the CIRP*, Vol. 46, pp. 287~290.

El-Khasawneh, B. S. and Ferreira, P. M., 1999, "Computation of Stiffness Bounds for Parallel Link Manipulators," *International Journal of Machine Tools & Manufacture*, pp. 321~342.

Gosselin, C., 1990, "Stiffness Mapping for Parallel Manipulator," *IEEE Transactions on Robotics and Automation*, Vol. 6, No. 3, pp. 377~382.

Ha, H. P., and Han, M. C., 2001, "A Fast Forward Kinematic Analysis of Stewart Platform," *Transactions of the KSME*, A, Vol. 25, No. 3, pp. 339~352.

Jeong, W. and Choi, Y. J., 1999, "Static Error Compensation for the Stewart Platform based Machine Tool," *Proceedings of the KSPE 1999 Autumn Annual Meeting*, Vol. 1, pp. 239~242.

Kim, T., Kim, H., and Hong, D., 2000, "Analysis of Stiffness for Parallel Devices Using Eigenvalues," *Proceedings of the KSPE 2000 Spring Annual Meeting*, Vol. 2, pp. 699~702.

Lim, S. R., Choi, W. C., Song, J. B., and Hong, D., 2001, "Effect of Joint Errors in a Cubic Parallel Device," *Journal of the KSPE*, Vol. 18, No. 6, pp. 87~92.

Masory, O. and Wang, J., 1993, "On the Accuracy of a Stewart Platform-Part I The Effect of Manufacturing Tolerances," *IEEE Conference on Robotics and Automation*, Vol. 1, pp. 114~120.

Ropponen, T. and Arai, T., 1995, "Accuracy Analysis of a Modified Stewart Platform Manipulator," *IEEE Conference on Robotics and Automation*, Vol. 1, pp. 521~525.

Satori, S. and Zhang, G. X., 1995, "Geometric Error Measurement and Compensation of Machines," *Annals of the CIRP*, Vol. 44, pp. 599~609.

Wang, S. M. and Ehmann, K. F., 1995, "Error Model and Accuracy Analysis of A Six-DOF Stewart Platform," *Manufacturing Science and Engineering*, Vol. 2, pp. 519~530.